Check for updates

Effects of vegetation lodging on overland runoff flow regime and resistance

Jingzhou Zhang, Shengtang Zhang, Guibao Li, Ming Liu and Si Chen

ABSTRACT

Vegetation is a vital part of the natural environment. Variations in vegetation morphology produce changes in the mechanical and fluid characteristics of overland flow. Determining the effects of vegetation lodging on the overland runoff flow regime and resistance is a prerequisite for accurately simulating overland runoff and convergence, revealing the mechanism of overland flow propagation, and the design and management of vegetation protection, soil consolidation, and ecological slope engineering. To systematically study the effects of vegetation lodging on overland runoff, four planting vegetation lodging angles (α) and 10 test water depths were used to simulate experimental research with a 1.0% slope ratio. Experimental results show that the depth and state of vegetation inundation and the degree of lodging significantly influence the flow regime and resistance. Under the same water depth, higher values of α are associated with higher values of the flow velocity, Reynolds number, Froude number, and Darcy–Weisbach resistance coefficient (f), and lower values of the drag coefficient (C_D). The overall result is enhanced turbulence in the flow field and weaker flow resistance. Numerical statistics and difference analysis indicate that, when the vegetation is non-submerged, a 10° increase in α produces a 9.30% decrease in f. In the submerged state, a 10° increase in α causes a 26.70% decrease in f. C_D is greatly affected by the boundary water depth. Below some critical water depths, an increase of 10° in α reduces C_D by 8.48%. Above the critical depth, a 10° increase in α decreases C_D by 41.10%.

Key words | flow regime, flow resistance, overland runoff, vegetation lodging

Jingzhou Zhang
Shengtang Zhang (corresponding author)
Guibao Li
Ming Liu
Si Chen
Shandong University of Science and Technology,
Qingdao 266590,
China
E-mail: *zst0077@163.com*

Shengtang Zhang
Key Laboratory of Hydraulic and Waterway Engineering of the Ministry of Education,
Chongqing Jiaotong University,
Chongqing, 400074,
China

INTRODUCTION

Vegetation is a vital component of the natural environment. As such, it is an important factor in maintaining the integrity and health of slope ecosystems, and has a very high ecological service value (Wang *et al.* 2015a, 2015b; Ding & Li 2016; Mohammadiun *et al.* 2016; Yasi & Ashori 2016; Zhang *et al.* 2018). The existence of slope vegetation can effectively reduce sediment transport and slow down the erosion process (Huthoff *et al.* 2007; Cheng & Nguyen 2011; Cheng *et al.* 2012; Zhang *et al.* 2014; Li *et al.* 2015; Vargas-Luna *et al.* 2015), while simultaneously increasing the overland slope resistance (Gabarrón-Galeote *et al.* 2013; Lieskovsky & Kenderessy 2014; Zhao *et al.* 2015; Li *et al.* 2018; Zhu *et al.* 2018). As a result, vegetation is widely used in slope protection, soil and water conservation, and other aspects of hydraulic design. However, studies of overland runoff are complicated by morphological changes in vegetation (Armanini *et al.* 2005; Wilson 2007), and so it is particularly important to study the turbulence and resistance mechanisms of overland runoff. This will provide a scientific basis for accurately simulating the process of slope production and convergence, identifying the mechanism of overland flow movement, predicting and controlling regional catastrophic floods, and designing and managing soil slope protection and ecological slope engineering.

doi: 10.2166/ws.2020.059

Downloaded from http://iwa.silverchair.com/ws/article-pdf/20/4/1463/704790/ws020041463.pdf
by guest

Vegetation can be characterized according to its flexibility or rigidity. For example, flexible vegetation plunges its roots into mud while the relative height of the vegetation is submerged in water. Thus, flexible vegetation can easily tilt and fall under the action of overland flow. Palmer (1945) studied the behavior of vegetation stems and leaves under three characteristic flow rates and different submergence states. The results showed that non-submerged aquatic plants did not bend under a low-speed water flow, whereas in the submerged state, the plants tended to bend in the direction of water flow during medium-speed water flow and tilt under a high-speed flow at a fixed oblique angle. These results are consistent with the findings of Carollo *et al.* (2005) and Busari & Li (2015). Kouwen *et al.* (1981) argued that the resistance of flexible plants to overland flow is also constrained by the shape of the plant itself and the flow regime. The concept of the bending stiffness of vegetation over a unit area was proposed, and a semi-empirical formula for Manning's roughness coefficient was derived using the empirical coefficient of deflection characteristics. Velasco *et al.* (2003) conducted experimental studies on various densities of flexible submerged vegetation. The results showed that vegetation roughness is directly related to the height offset value, relative roughness is negatively correlated with flow rate, and its resistance coefficient tends to a certain value. These conclusions are similar to those of Cantalice *et al.* (2013), who found that the flow resistance decreases after plant deflection in the non-submerged state, and Schoelynck *et al.* (2013), who concluded that vegetation under the impact of water flow will be deformed into a streamlined shape to reduce the resistance. Armanini *et al.* (2005) argued that under non-submerged conditions plant deflection does not result in a change in the water-blocking area, and so the water flow resistance coefficient can be assumed to be constant.

Although the hydrodynamic characteristics of vegetation lodging have been studied, there are still many areas that need to be explored in greater depth (Velasco *et al.* 2003; Li *et al.* 2014; Busari & Li 2015; Han *et al.* 2016). The effect of vegetation lodging on the overland flow field complicates the flow turbulence and resistance law. Research on the complexity of the overland flow characteristics and the hysteresis of the measurement technique under lodging conditions is relatively undeveloped (Järvelä 2002; Carollo *et al.* 2005; Wang *et al.* 2015a, 2015b). The effect and extent of vegetation lodging changes the resistance characteristics of the flow, resulting in a significant stagnant sand retention effect and a certain impact on the slope production and convergence. To accurately describe this effect, it is necessary to conduct an in-depth study of the flow characteristics of this particular fluid.

In this paper, the hydrodynamic characteristics of water flowing overland under the action of vegetation lodging are systematically studied by combining vegetation discharge simulations with the theory of fluid mechanics. Variations in the vegetation lodging degree and submergence under different water depth conditions are analyzed to clarify the differences between the flow characteristics and resistance characteristics, thus promoting the expansion of open-channel hydraulics theory to overland flow through vegetation. Moreover, this research lays the theoretical foundations for studies on the mechanism by which vegetation blocks the transport of water and sediment.

METHODS AND MATERIALS

Design of the experimental installation

The overland flow study reported here mainly used the basic theory of flow in an open channel (Hsieh 1964; Li & Shen 1973). Many studies on the effects of vegetation on a slope during water erosion have used variable slopes involving rectangular flume experiments. To enhance the experimental effect and improve the efficiency, single-plant vegetation was generalized into an effective water-blocking cylinder in the experiment (Huthoff *et al.* 2007; Yagci *et al.* 2010). The structure of the test tank is shown in Figure 1. The following design points were determined according to the purpose of the test:

(1) The test area was a polymethyl methacrylate flume with a slope of 1.0% that is divided into three sections: an upstream flat water section, an experimental procedure section, and a downstream water measuring section. The structural dimensions of the test plot were 5.0 m long, 0.4 m wide, and 0.3 m high.
(2) Light aluminum cylindrical rods were used to simulate the vegetation. The height of the simulated vegetation was set at 0.1 m and the stem diameter was 0.004 m.

Downloaded from http://iwa.silverchair.com/ws/article-pdf/20/4/1463/704790/ws020041463.pdf
by guest

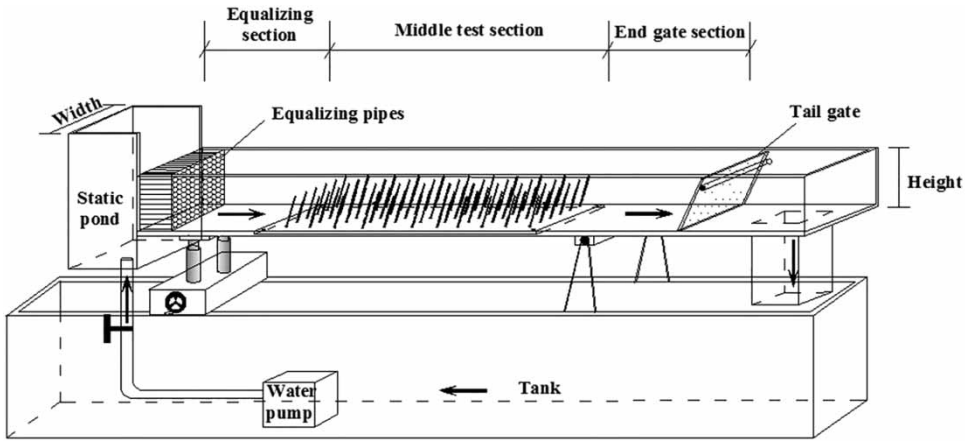

Figure 1 | Experimental apparatus figure.

Combined with the height of the test structure, the lodging angle α was set to 20°, 40°, 60°, or 80° in each of the four working conditions (as shown in Figure 2), and the adjacent vegetation was uniformly arranged over an area of $0.06 \times 0.06\ m^2$.

(3) To systematically study the internal relationship between the vegetation inundation state and vegetation lodging angle (i.e. quantitative analysis of water depth and lodging angle), the final design was subjected to 10 test treatments in which the water depth ranged from 0.01 to 0.10 m at intervals of 0.01 m.

(4) Two longitudinal observation sections were set up from top to bottom along the experimental laying section with a spacing of 1.5 m. Three measuring points were set for each observation section, and the velocity and water depth of each section were observed. The lateral measuring point was positioned between two plants to avoid the high and low points of the water surface in the drop zone of the vegetation wake, thus minimizing the influence of lateral variations in the flow velocity on the test results.

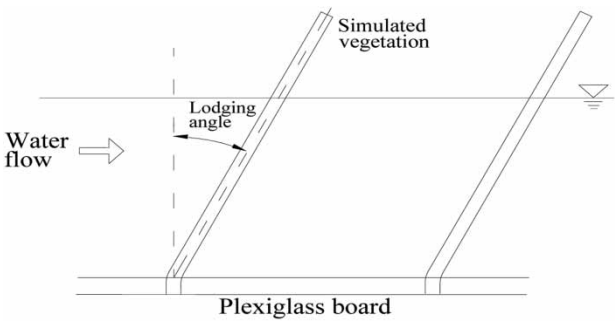

Figure 2 | Ematic diagram of vegetation lodging state.

Hydraulic parameter calculation

(1) Overland runoff is typically analyzed by measuring flow properties, flow velocity, erosion caused by the flow, and sediment transportation. Two important hydraulic parameters are the Reynolds number (*Re*) and Froude number (*Fr*) (Horton *et al.* 1934; Woolhiser *et al.* 1970; Sidorchuk *et al.* 2008).

The mechanical significance of *Fr* lies in determining the ratio of the inertial force of the flow due to gravity. From an energy perspective, *Fr* represents the ratio of average kinetic energy per unit weight of a liquid to the average potential energy. For open-channel flow,

$$Fr = \frac{V}{\sqrt{gh}} \tag{1}$$

where V is the water velocity (m/s), h is the water depth (m), and g is the acceleration due to gravity (m/s^2).

Re is an essential parameter used to reflect flow patterns. This important parameter measures the ratio of the inertial force of a viscous fluid flow to the viscous force. Inertial forces act as a disturbance to the body of water, causing it to break away from regular motion. Viscous forces weaken the effect of blocking

Downloaded from http://iwa.silverchair.com/ws/article-pdf/20/4/1463/704790/ws020041463.pdf
by guest

the disturbance and maintaining the regular flow. *Re* can be calculated as

$$Re = \frac{VR}{v} \tag{2}$$

where v is the motion viscosity coefficient (m^2/s) and R is the hydraulic radius. Using the Poiseuille formula,

$$v = 0.01775/(1 + 0.337T + 0.00022T^2) \tag{3}$$

where T is the temperature of the water (°C).

(2) Resistance is the retardation effect that the vegetation and roughness of the surface of the ground impose on the water flow. Studying the flow resistance is an integral part of investigations into overland flow (Weltz *et al.* 1992; Barros & Colello 2001). In this study, the Darcy–Weisbach resistance coefficient (f) and the drag coefficient (C_D) reflect the overall underlying surface resistance and vegetation flow resistance characteristics, respectively. Generally speaking, the overland flow resistance is composed of the surface roughness, flow around the vegetation, internal flow retardation, and boundary effects, and thus reflects the effect of the overall underlying surface on flow resistance (Zhang *et al.* 2010; Wang *et al.* 2014). C_D reflects the resistance of the vegetation on the flow (Liu *et al.* 2008; Cheng 2013; Liu & Zeng 2016). If the overland flow friction factor can be calculated precisely, the mechanism by which the overland flow varies may be better understood (Zheng *et al.* 2012). The Darcy–Weisbach resistance coefficient, f, is expressed as follows:

$$f = \frac{8h_f Rg}{LV^2} \tag{4}$$

where h_f is the frictional head loss (m) and L is the length of the test section (m). C_D is expressed as follows:

$$C_D = \frac{(1-\lambda)^2 \pi g d R}{2\lambda V^2} \tag{5}$$

where π is equal to 3.14, d is the stem roughness (m), and λ is the coverage per unit area, calculated as:

$$\lambda = \frac{1}{L^2}\frac{\pi d^2}{4} \tag{6}$$

where L is the distance between adjacent plants (m).

The experimental calculation data corresponding to the different values of α are presented in Table 1.

EXPERIMENTAL RESULTS AND ANALYSES

Flow pattern and regime

The pattern and regime of the overland flow are determined in terms of open-channel two-dimensional flow, whereby the flow pattern can be divided into a laminar flow zone, transition zone, and turbulent flow zone. The turbulent zone can be subdivided into a turbulent smooth zone, turbulent transition zone, and turbulent rough zone. The law of flow resistance is different in different flow zones, and *Re* is an important indicator for judging the flow pattern. The flow pattern is generally divided into laminar flow, transitional flow, and turbulent flow. The flow regime refers to whether the vegetation water flow is slow or rapid. Generally, there are three kinds of flow states, namely slow flow, critical flow, and rapid flow.

According to the above analysis, the flow can be divided into six flow states: (1) slow laminar flow, (2) slow transitional flow, (3) slow turbulent flow, (4) rapid laminar flow, (5) rapid transient flow, and (6) rapid turbulent flow. Let us approximate $v = 1 \times 10^{-6}\,m^2/s$ and take the hydraulic radius $R = h$. Then, finding simultaneous solutions to $Re = VR/v$ and $Fr = V/\sqrt{gh}$ and plotting them in the logarithmic coordinates of water depth h and average flow velocity V, we obtain two clusters of parallel lines where *Re* and *Fr* are constant, respectively. The values $Re = 500$, $Re = 5{,}000$, and $Fr = 1$ are used as the boundaries, and the six-zone flow regime can be determined.

Figure 3 plots the flow regime under the various test conditions. As can be seen from Figure 3, an increase in water depth produces an upward trend in the average velocity of water flow. The reason is shown in Figures 4 and 5. The water depth is positively correlated with *Re* and negatively correlated with *Fr*. As the water depth increases, the inertial force of the fluid dominates the viscous force and the average potential energy; this result is complementary to the conclusions of Li *et al.* (2013). When the vegetation is in the non-submerged state, the rate of increase in velocity is small; however, when the vegetation is completely submerged, the rate of increase in velocity gradually rises.

Downloaded from http://iwa.silverchair.com/ws/article-pdf/20/4/1463/704790/ws020041463.pdf
by guest

Table 1 | Experimental data of hydraulic parameters of four different vegetation lodging angles

Lodging angle α	Parameter	Experiment number 1	2	3	4	5	6	7	8	9	10
20°	h (m/s)	0.01	0.02	0.03	0.04	0.05	0.06	0.07	0.08	0.09	0.10
	V (m/s)	0.2390	0.2461	0.2474	0.2433	0.2457	0.2509	0.2589	0.2687	0.2798	0.2935
	Fr	0.8083	0.6064	0.4599	0.3903	0.3537	0.3279	0.3128	0.3035	0.2982	0.2965
	Re	10,317	20,231	29,234	36,824	44,649	52,738	61,158	70,002	79,155	89,195
	f	0.1104	0.1233	0.1300	0.1551	0.1989	0.2384	0.2612	0.2833	0.2869	0.2688
	C_D	2.7959	1.8296	1.1497	1.0426	1.1100	1.1583	1.1279	1.1095	1.0358	0.9017
	Submerged state	■	■	■	■	■	■	■	■	□	□
40°	h (m/s)	0.01	0.02	0.03	0.04	0.05	0.06	0.07	0.08	0.09	0.10
	V (m/s)	0.2462	0.2528	0.2595	0.2554	0.2549	0.2612	0.2676	0.2799	0.2943	0.3057
	Fr	0.8298	0.6657	0.5016	0.4087	0.3644	0.3419	0.3231	0.3163	0.3134	0.3088
	Re	10,611	20,634	30,658	38,659	46,395	54,857	63,217	72,929	83,239	92,887
	f	0.1016	0.1068	0.1119	0.1218	0.1550	0.1906	0.2145	0.2113	0.1896	0.1699
	C_D	2.6778	1.8864	1.0950	0.8214	0.8665	0.9258	0.9258	0.8302	0.6838	0.5228
	Submerged state	▲	▲	▲	▲	▲	▲	△	△	△	△
60°	h (m/s)	0.01	0.02	0.03	0.04	0.05	0.06	0.07	0.08	0.09	0.10
	V (m/s)	0.2543	0.2612	0.2681	0.2594	0.2614	0.2698	0.2796	0.2934	0.3051	0.3170
	Fr	0.8797	0.6970	0.5142	0.4148	0.3739	0.3531	0.3377	0.3315	0.3250	0.3200
	Re	10,919	21,284	31,649	39,254	47,551	56,667	66,016	76,365	86,265	96,274
	f	0.0882	0.0898	0.0914	0.0933	0.1081	0.1173	0.1115	0.0937	0.0816	0.0725
	C_D	2.4668	1.6280	0.7891	0.6285	0.6051	0.5749	0.4825	0.3671	0.2948	0.2417
	Submerged state	●	●	●	●	●	○	○	○	○	○
80°	h (m/s)	0.01	0.02	0.03	0.04	0.05	0.06	0.07	0.08	0.09	0.10
	V (m/s)	0.2621	0.2780	0.2872	0.2885	0.2876	0.2918	0.2997	0.3081	0.3184	0.3325
	Fr	0.8954	0.6616	0.5397	0.4624	0.4110	0.3809	0.3619	0.3480	0.3391	0.3350
	Re	11,402	22,986	33,874	43,536	52,263	61,232	70,716	80,146	90,004	100,877
	f	0.0681	0.0725	0.0731	0.0640	0.0592	0.0590	0.0509	0.0362	0.0265	0.0248
	C_D	2.3502	1.4341	0.7554	0.3545	0.2962	0.2948	0.2199	0.2077	0.0955	0.0818
	Submerged state	×	×	*	*	*	*	*	*	*	*

Note: ■ is 20° non-submerged point, □ is 20° submerged point, ▲ is 40° non-submerged point, △ is 40°submerged point, ● is 60° non-submerged point, ○ is 60° submerged point, × is 80° non-submerged point, and * is 80° non-submerged point.

Downloaded from http://iwa.silverchair.com/ws/article-pdf/20/4/1463/704790/ws020041463.pdf
by guest

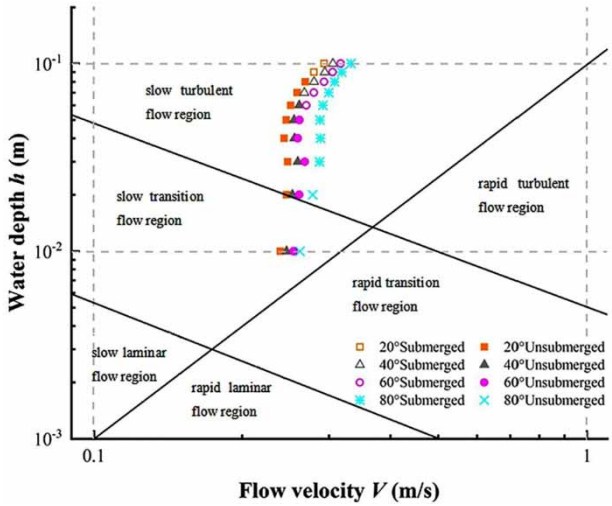

Figure 3 | Flow regime partition diagram under different lodging conditions.

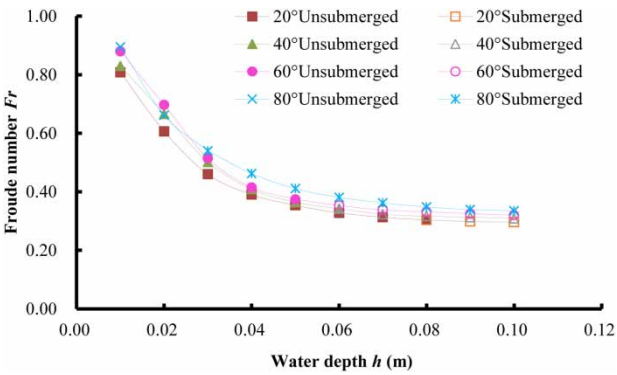

Figure 4 | *h–Fr* relation curves under different lodging conditions.

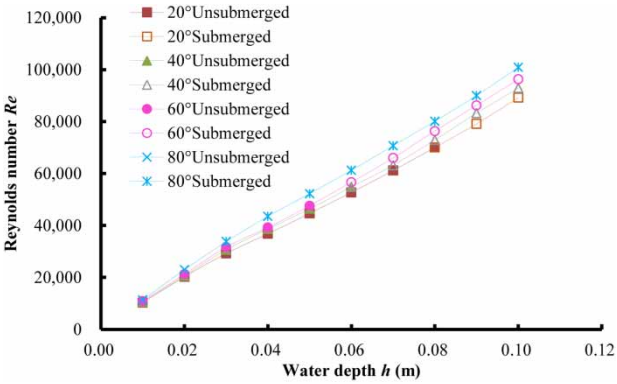

Figure 5 | *h–Re* relation curves under different lodging conditions.

This may be because the completely submerged vegetation reduces the flow resistance. It can be seen from Figures 6 and 7 that when the vegetation is submerged, f and C_D

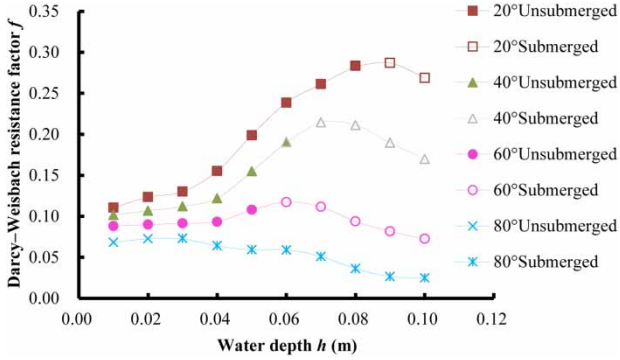

Figure 6 | *h–f* relation curves under different lodging conditions.

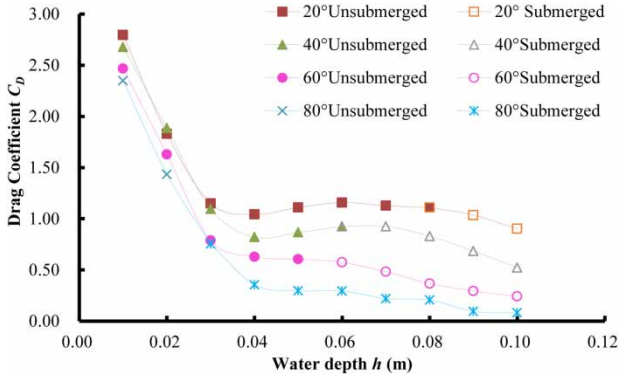

Figure 7 | *h–C*$_D$ relation curves under different lodging conditions.

decrease as the water depth increases. This decrease in the overall flow resistance of the underlying surface and vegetation ensures the smooth flow of overland fluid and increases the velocity. Under the test conditions, the flow regime is in the slow transition flow and slow turbulent flow regions. As the water depth increases, the proportion of fluid inertial force gradually becomes greater than the viscous force (see Figure 5). The turbulence of the flow destabilizes the flow field, causing the flow regime to move from the slow transition regime to slow turbulent flow.

It can also be seen from Figure 3 that for the same water depth condition, a larger vegetation lodging angle α results in a greater flow velocity V. The reason is inseparable from the flow regime and flow resistance response. Under the same water depth conditions, Figures 4 and 5 show that $Fr_{20^\circ} < Fr_{40^\circ} < Fr_{60^\circ} < Fr_{80^\circ}$ and $Re_{20^\circ} < Re_{40^\circ} < Re_{60^\circ} < Re_{80^\circ}$, respectively. This indicates that a larger vegetation lodging angle results in a greater kinetic energy and inertia force in the flowing water body and a smaller average

Downloaded from http://iwa.silverchair.com/ws/article-pdf/20/4/1463/704790/ws020041463.pdf
by guest

potential energy and viscous force. The overall result is a larger flow velocity and stronger flow turbulence.

Under the same water depth conditions, Figures 6 and 7 show that $f_{20^\circ} > f_{40^\circ} > f_{60^\circ} > f_{80^\circ}$ and $C_{D20^\circ} > C_{D40^\circ} > C_{D60^\circ} > C_{D80^\circ}$, respectively. The larger the lodging angle of the vegetation, the smaller the corresponding f and C_D values, and a lower water-blocking capacity leads to an increase in the flow capacity. Both the flow regime and the resistance response explain why a larger vegetation lodging angle has a larger corresponding flow velocity.

In general, the flow pattern of the water changes from the slow transition to the slow turbulent flow as the water depth increases. At the same time, as the vegetation lodging angle increases, the turbulence of the flow strengthens. These are important factors affecting the flow regime.

Resistance characteristics

Flow resistance refers to the roughness of the bed surface and the blocking effect of vegetation on the flow of water. The resistance to overland flow is often represented by the hydraulic roughness coefficient (Smith *et al.* 2007). Most scholars use the Darcy–Weisbach resistance coefficient f and the drag coefficient C_D to characterize the resistance. For most slopes containing vegetation, the dominant component of flow resistance is assumed to be generated by coarse vegetation, and so the comprehensive resistance of overland flow can be replaced by vegetation resistance. However, the comprehensive flow resistance is mainly composed of the circumfluence resistance, boundary resistance, or particle resistance generated by the flow through the vegetation. There are many influencing factors, making it difficult to accurately simulate the hydraulic characteristics of overland flow using suitable approximations. This study therefore systematically compared the composite resistance f and the vegetation flow resistance C_D to determine the change in comprehensive resistance caused by vegetation flow.

Figure 6 illustrates the relation between h and f under four different lodging states. There is a critical water depth ($h = 0.03$ m) below which the test points are mostly non-submerged. In this domain, f increases with h, albeit relatively gently. When h is greater than the critical depth, f increases with h in the non-submerged state, but decreases as h increases in the fully submerged state. The peak value of f is attained when the vegetation is just completely submerged. This conclusion is consistent with the research results of Armanini *et al.* (2005) regarding the flow resistance of flexible vegetation. It can be inferred that, under the non-submerged condition, increasing the water depth effectively increases the solid interface between the water body and the bottom boundary, the lateral boundary, and the vegetation. This increases the solid–liquid contact and the collision probability. Therefore, the frictional resistance under the corresponding conditions increases, resulting in an increase in the comprehensive resistance of the flow. As the vegetation becomes completely submerged, the solid–liquid contact ratio decreases with any further increase in the water depth, so that the comprehensive resistance of the flow gradually decreases.

Figure 7 plots the relation between h and C_D under four different lodging states. Again, there is a critical water depth ($h = 0.03$ m) below which C_D decreases rapidly with water depth. When h is greater than the boundary water depth, C_D rises slowly with the water depth in the non-submerged state, but declines slowly with the water depth in the submerged state. The overall law is consistent with the research results of Ishikawa *et al.* (2000). The experimental phenomenon suggests that when the initial water depth is small ($h = 0.01$ m), the overland flow covers the entire test floor to form a thin layer of flow. Under the action of surface tension, the extremely thin flow is fully in contact with the solid surface of vegetation, test floor, and air, making the three-phase solid–liquid–gas medium heavily doped. The vegetation therefore has a water-blocking and circumfluence effect on the thin-layer flow. In this way, a backwater wave of a certain height is formed upstream of the vegetation, and the flow lines on the back surfaces separate to form a wake vortex. This increases the degree of undulation of the free surface of the fluid and increases the resistance of the vegetation to the water flow, resulting in a larger C_D. Below the critical depth, an increase in the water depth strengthens the turbulence of the flow, and the momentum exchange inside the liquid promotes the uniformity of the velocity distribution. In this case, the ratio of solid and air doping in the solid–liquid–gas medium is greatly reduced, and the subsequent decrease in backwater and wake intensity leads to a rapid decrease in C_D. When the water depth exceeds the

Downloaded from http://iwa.silverchair.com/ws/article-pdf/20/4/1463/704790/ws020041463.pdf
by guest

Table 2 | The change rate of the Darcy–Weisbach resistance coefficient f under different lodging conditions in non-submerged states

	Experiment number									
Parameter	**1**	**2**	**3**	**4**	**5**	**6**	**7**	**8**	**9**	**10**
h (m/s)	0.01	0.02	0.03	0.04	0.05	0.06	0.07	0.08	0.09	0.10
f_{20°	0.1104	0.1233	0.1300	0.1551	0.1989	0.2384	0.2612	0.2833	–	–
f_{40°	0.1016	0.1068	0.1119	0.1218	0.1550	0.1906	–	–	–	–
f_{60°	0.0882	0.0898	0.0914	0.0933	0.1081	–	–	–	–	–
f_{80°	0.0681	0.0725	–	–	–	–	–	–	–	–
$(f_{40^\circ} - f_{20^\circ})/f_{20^\circ}$	−8.04%	−13.42%	−13.90%	−21.43%	−22.10%	−20.05%	–	–	–	–
$(f_{60^\circ} - f_{40^\circ})/f_{40^\circ}$	−13.20%	−15.89%	−18.33%	−23.40%	−30.26%	–	–	–	–	–
$(f_{80^\circ} - f_{60^\circ})/f_{60^\circ}$	−22.71%	−19.21%	–	–	–	–	–	–	–	–

critical depth, the contact area between the vegetation and the flow increases with h under the non-submerged condition, and f increases slowly. Once the vegetation is submerged, the behavior is completely the opposite.

Both Figures 6 and 7 give the same critical depth of water, but there are still differences between the two kinds of flow resistance with water depth. The reason may be related to the composition of flow resistance. As mentioned earlier, f reflects the effect of the overall underlying surface on comprehensive flow resistance. The experimental conditions mainly include boundary resistance and vegetation resistance, and neglect particle resistance. C_D only reflects the effect of vegetation on flow resistance. When h is less than the critical depth, that is, the thin-layer flow is spread out across the whole slope, the boundary effect of the fluid increases under the action of surface tension, and the vegetation resistance decreases under the influence of the flow structure. Figure 6 shows that f increases slowly with h below the critical depth. This further shows that boundary resistance is the main flow resistance and that vegetation resistance is secondary. Moreover, the increment in boundary resistance is greater than that of vegetation resistance. When the water depth exceeds the critical water depth, the boundary effect of the slope is weakened and the vegetation resistance is enhanced. Figures 6 and 7 also suggest that under the same water depth, a larger lodging angle is associated with smaller corresponding f and C_D values and lower water-resisting capacity. In fact, the average velocity and resistance are two expressions of the same problem.

From the above analysis, it can be seen that the flow resistance characteristics of lodging vegetation are mainly related to the degree of lodging, the submerged state of vegetation, and the boundary water depth. Under the same water depth, larger lodging angles give smaller f and C_D and weaker water-resisting ability, which is consistent with the conclusion of Schoelynck *et al.* (2013). The Darcy–Weisbach resistance coefficient, f, is greatly affected by vegetation submergence. Through numerical statistics and difference analysis (Tables 2 and 3), it can be concluded that when the vegetation is in the non-submerged state, every 10° increase in lodging angle produces a decrease of 9.30% in f. In the submerged state, every 10° increase in lodging angle causes f to decrease by 26.70%. C_D is greatly influenced by the critical depth of water. Numerical statistics and difference analysis (Table 4) show that an increase of 10° in the lodging angle produces a decrease in C_D of 8.48% (below critical water depth) and 41.10% (above the critical depth).

CONCLUSIONS

Vegetation lodging can change the regime and resistance characteristics of overland flow. To investigate the flow characteristics of this special flow type, this study conducted various experimental simulations. The following conclusions can be stated:

(1) Under the given test conditions, the water depth and lodging angle are important factors affecting the flow

Downloaded from http://iwa.silverchair.com/ws/article-pdf/20/4/1463/704790/ws020041463.pdf
by guest

Table 3 | The change rate of the Darcy–Weisbach resistance coefficient f under different lodging conditions in submerged states

	Experiment number									
Parameter	**1**	**2**	**3**	**4**	**5**	**6**	**7**	**8**	**9**	**10**
h (m/s)	0.01	0.02	0.03	0.04	0.05	0.06	0.07	0.08	0.09	0.10
f_{20°	–	–	–	–	–	–	–	–	0.2869	0.2688
f_{40°	–	–	–	–	–	–	0.2145	0.2113	0.1896	0.1699
f_{60°	–	–	–	–	–	0.1173	0.1115	0.0937	0.0816	0.0725
f_{80°	–	–	0.0731	0.0640	0.0592	0.0590	0.0509	0.0362	0.0265	0.0248
$(f_{40^\circ} - f_{20^\circ})/f_{20^\circ}$	–	–	–	–	–	–	–	–	−33.91%	−36.79%
$(f_{60^\circ} - f_{40^\circ})/f_{40^\circ}$	–	–	–	–	–	–	−48.02%	−55.66%	−56.94%	−57.34%
$(f_{80^\circ} - f_{60^\circ})/f_{60^\circ}$	–	–	–	–	–	−49.71%	−54.37%	−61.30%	−67.60%	−65.82%

Table 4 | The change rate of the drag coefficient C_D under different lodging conditions

	Experiment number									
	$h \leq$ Critical depth of water			$h >$ Critical depth of water						
Parameter	**1**	**2**	**3**	**4**	**5**	**6**	**7**	**8**	**9**	**10**
h (m/s)	0.01	0.02	0.03	0.04	0.05	0.06	0.07	0.08	0.09	0.10
C_{D20°	2.7959	1.8296	1.1497	1.0426	1.1100	1.1583	1.1279	1.1095	1.0358	0.9017
C_{D40°	2.6778	1.8864	1.0950	0.8214	0.8665	0.9258	0.9258	0.8302	0.6838	0.5228
C_{D60°	2.4668	1.6280	0.7891	0.6285	0.6051	0.5749	0.4825	0.3671	0.2948	0.2417
C_{D80°	2.3502	1.4341	0.7554	0.3545	0.2962	0.2948	0.2199	0.2077	0.0955	0.0818
$(C_{D20^\circ} - C_{D40^\circ})/C_{D40^\circ}$	4.41%	−3.01%	4.99%	26.92%	28.10%	25.11%	21.82%	33.63%	51.47%	72.48%
$(C_{D40^\circ} - C_{D60^\circ})/C_{D60^\circ}$	8.55%	15.87%	38.76%	30.71%	43.20%	61.02%	91.86%	126.17%	131.97%	116.27%
$(C_{D60^\circ} - C_{D80^\circ})/C_{D80^\circ}$	4.96%	13.52%	4.47%	77.28%	104.28%	95.01%	119.46%	76.71%	208.80%	195.66%

regime. V and Re are positively correlated with h, whereas Fr is negatively correlated with h. As the water depth increases, the flow regime changes from slow transition flow to slow turbulence flow. For the same water depth, a larger lodging angle results in larger values of V, Fr, and Re, and stronger turbulence in the flow.

(2) The flow resistance characteristics of lodging vegetation are related to the degree of vegetation lodging, submerged state, and critical water depth. The relations between f, C_D, and h indicate the same critical water depth, but there are still differences between how the flow resistance varies with water depth. In the non-submerged state, f is positively correlated with h, whereas in the submerged state, it is negatively correlated. C_D decreases rapidly with h when it is below the critical depth, whereas the submerged vegetation plays a greater role when h is above the critical depth, but C_D changes steadily with h.

(3) At the same water depth, a larger lodging angle produces smaller values of f and C_D and weaker water resistance. The Darcy–Weisbach resistance coefficient, f, is greatly affected by vegetation submergence. Statistical analysis of the numerical difference shows that in the non-submerged state, f will decrease by 9.30% for every 10° increase in the lodging angle; in the submerged state, f decreases by 26.70% for every 10° increase in lodging angle. C_D is greatly affected by the critical water depth. Up to the critical depth, when the lodging angle increases by 10°, C_D will decrease by 8.48%. When h

Downloaded from http://iwa.silverchair.com/ws/article-pdf/20/4/1463/704790/ws020041463.pdf
by guest

is greater than the critical depth, every 10° increase in lodging angle causes C_D to decrease by 41.10%.

Note that these conclusions are based on the premise of controlling for other influencing factors. To simplify the study, this experiment unified the simulated vegetation height and lodging angle. However, in reality, the slope surface is complex and changeable, and the elastic modulus of vegetation leads to different morphological characteristics, as well as bending and swinging under the action of water flow, and so the mechanism of water flow needs to be further explored. In addition, the effect of the movement of vegetation on overland flow is a multidisciplinary problem, and the transport of sediment, pollutants, and organisms should be considered. It is therefore necessary to further study the influence of slope vegetation on the transport characteristics of sediment and pollutants. The reliability and adaptability of these conclusions should also be explored in further detail.

ACKNOWLEDGEMENTS

The authors would like to thank the National Natural Science Foundation of China (Grant no. 41471025), the Natural Science Foundation of Shandong Province (Grant no. ZR2017MEE055), and the Major Research and Development Program of Shandong Province (Grant no. 2016GSF117027 and 2016GSF117036) for supporting this project.

REFERENCES

Armanini, A., Righetti, M. & Grisenti, P. 2005 Direct measurement of vegetation resistance in prototype scale. *Journal of Hydraulic Research* **43** (5), 481–487.

Barros, A. P. & Colello, J. D. 2001 Surface roughness for shallow overland flow on crushed stone surfaces. *Journal of Hydraulic Engineering ASCE* **127** (1), 38–52.

Busari, A. O. & Li, C. W. 2015 A hydraulic roughness model for submerged flexible vegetation with uncertainty estimation. *Journal of Hydro-Environment Research* **9** (2), 268–280.

Cantalice, J. R. B., Melo, R. O., Silva, Y. J. A. B., Cunha Filho, M., Araújo, A. M., Vieira, L. P., Bezerra, S. A., Barros Jr., G. & Singh, V. P. 2013 Hydraulic roughness due to submerged, emergent and flexible natural vegetation in a semiarid alluvial channel. *Journal of Arid Environments* **114** (Feb), 1–7.

Carollo, F. G., Ferro, V. & Termini, D. 2005 Flow resistance law in channels with flexible submerged vegetation. *Journal of Hydraulic Engineering* **131** (7), 554–564.

Cheng, N. S. 2013 Calculation of drag coefficient for arrays of emergent circular cylinders with pseudo fluid model. *Journal of Hydraulic Engineering* **139** (6), 602–611.

Cheng, N. S. & Nguyen, H. T. 2011 Hydraulic radius for evaluating resistance induced by simulated emergent vegetation in open-channel flows. *Journal of Hydraulic Engineering* **137** (9), 995–1004.

Cheng, N. S., Nguyen, H. T., Tan, S. K. & Shao, S. D. 2012 Scaling of velocity profiles for depth-limited open channel flows over simulated rigid vegetation. *Journal of Hydraulic Engineering* **138** (8), 673–683.

Ding, W. F. & Li, M. 2016 Effects of grass coverage and distribution patterns on erosion and overland flow hydraulic characteristics. *Environmental Earth Sciences* **75** (6), 1–14.

Gabarrón-Galeote, M. A., Martínez-Murillo, J. F., Quesada, M. A. & Ruiz-Sinoga, J. D. 2013 Seasonal changes in the soil hydrological and erosive response depending on aspect, vegetation type and soil water repellency in different mediterranean micro environments. *Solid Earth* **4** (4), 497–509.

Han, L. J., Zeng, Y., Chen, L. & Huai, W. 2016 Lateral velocity distribution in open channels with partially flexible submerged vegetation. *Environmental Fluid Mechanics* **16** (6), 1267–1282.

Horton, R. E., Leach, H. R. & Vliet, R. V. 1934 Laminar sheet-flow. *Transactions American Geophysical Union* **15** (2), 393–404.

Hsieh, T. 1964 Resistance of cylinder piers in open-channel flow. *Journal of Hydraulics Division* **90** (1), 161–173.

Huthoff, F., Augustijn, D. C. M. & Hulscher, S. J. M. H. 2007 Analytical solution of the depth-averaged flow velocity in case of submerged rigid cylindrical vegetation. *Water Resources Research* **43** (6), 129–148.

Ishikawa, Y., Mizuhara, K. & Ashida, S. 2000 Effect of density of trees on drag exerted on trees in river channels. *Journal of Forestry Research* **5** (4), 271–279.

Järvelä, J. 2002 Flow resistance of flexible and stiff vegetation: a flume study with natural plants. *Journal of Hydrology* **269** (1–2), 44–54.

Kouwen, N., Li, R. M. & Simons, D. B. 1981 Flow resistance in vegetated waterways. *Transactions of the ASABE* **24** (3), 0684–0690.

Li, R. M. & Shen, H. W. 1973 Effect of tall vegetation on flow and sediment. *Journal of Hydraulics Division* **99** (5), 793–814.

Li, G., Wang, X., Zhao, X., Huang, E., Liu, X. & Cao, S. 2013 Flexible and rigid vegetation in overland flow resistance. *Transactions of the ASABE* **56** (3), 919–926.

Li, Y. P., Wang, Y., Anim, D. O., Tang, C. Y., Du, W., Ni, L. X., Yu, Z. B. & Acharya, K. 2014 Flow characteristics in different densities of submerged flexible vegetation from an open-channel flume study of artificial plants. *Geomorphology* **204** (1), 314–324.

Downloaded from http://iwa.silverchair.com/ws/article-pdf/20/4/1463/704790/ws020041463.pdf
by guest

Li, H., Li, Z., Li, Z., Yu, J. & Liu, B. 2015 Evaluation of ecosystem services: a case study in the middle reach of the Heihe River Basin, Northwest China. *Physics and Chemistry of The Earth* **89–90**, 40–45.

Li, N., Sack, D., Gao, G., Liu, L. & Li, D. 2018 Holocene *Artemisia*-Chenopodiaceae-dominated grassland in North China: real or imaginary? *Holocene* **28**, 834–841.

Lieskovsky, J. & Kenderessy, P. 2014 Modelling the effect of vegetation cover and different tillage practices on soil erosion in vineyards: a case study in Vráble (Slovakia) using WATEM/SEDEM. *Land Degradation & Development* **25** (3), 288–296.

Liu, X. G. & Zeng, Y. H. 2016 Drag coefficient for rigid vegetation in subcritical open channel. *Procedia Engineering* **154**, 1124–1131.

Liu, D., Diplas, P., Fairbanks, J. D. & Hodges, C. C. 2008 An experimental study of flow through rigid vegetation. *Journal of Geophysical Research Earth Surface* **113** (F4), 1–16.

Mohammadiun, S., Neyshabouri, S. A. A. S., Naser, G. & Vahabi, H. 2016 Numerical investigation of submerged vane effects on flow pattern in a 90 junction of straight and bend open channels. *Iranian Journal of Science & Technology Transactions of Civil Engineering* **40** (4), 1–17.

Palmer, V. J. 1945 A method for designing vegetated water ways. *Agricultural Engineering* **26** (12), 516–520.

Schoelynck, J., Meire, D., Bal, K., Buis, K., Troch, P., Bouma, T., Meire, P. & Temmerman, S. 2013 Submerged macrophytes avoiding a negative feedback in reaction to hydrodynamic stress. *Limnologica – Ecology and Management of Inland Waters* **43** (5), 371–380.

Sidorchuk, A., Schmidt, J. & Cooper, G. 2008 Variability of shallow overland flow velocity and soil aggregate transport observed with digital videography. *Hydrological Processes* **22** (20), 4035–4048.

Smith, M. W., Cox, N. J. & Bracken, L. J. 2007 Applying flow resistance equations to overland flows. *Progress in Physical Geography* **31**, 363–387.

Vargas-Luna, A., Crosato, A. & Uijttewaal, W. S. J. 2015 Effects of vegetation on flow and sediment transport: comparative analyses and validation of predicting models. *Earth Surface Processes & Landforms* **40** (2), 157–176.

Velasco, D., Bateman, A., Redondo, J. M. & Demedina, V. 2003 An open channel flow experimental and theoretical study of resistance and turbulent characterization over flexible vegetated linings. *Flow, Turbulence and Combustion* **70** (1–4), 69–88.

Wang, X. K., Yan, X. F., Zhou, S. F., Huang, E. & Liu, X. N. 2014 Longitudinal variations of hydraulic characteristics of overland flow with different roughness. *Journal of Hydrodynamics* **26** (1), 66–74.

Wang, W. J., Huai, W. X., Zeng, Y. H. & Zhou, J. F. 2015a Analytical solution of velocity distribution for flow through submerged large deflection flexible vegetation. *Applied Mathematics and Mechanics (English Edition)* **36** (1), 107–120.

Wang, K., Zhang, L., Qiu, Y., Ji, L. & Tian, F. 2015b Snow effects on alpine vegetation in the Qinghai–Tibetan Plateau. *Journal of Digital Earth* **8** (1), 56–73.

Weltz, M. A., Arslan, A. B. & Lane, L. J. 1992 Hydraulic roughness coefficients for native rangelands. *Journal of Irrigation and Drainage Engineering* **118** (5), 776–790.

Wilson, C. A. M. E. 2007 Flow resistance models for flexible submerged vegetation. *Journal of Hydrology* **342** (3), 213–222.

Woolhiser, D. A., Hanson, C. L. & Kuhlman, A. R. 1970 Overland flow on rangeland watersheds. *Journal of Hydrology New Zealand* **9**, 336–356.

Yagci, O., Tschiesche, U. & Kabdasli, M. S. 2010 The role of different forms of natural riparian vegetation on turbulence and kinetic energy characteristics. *Advances in Water Resources* **33** (5), 601–614.

Yasi, M. & Ashori, M. 2016 Environmental flow contributions from inbasin rivers and dams for saving Urmia lake. *Iranian Journal of Science and Technology – Transactions of Civil Engineering* **41** (1), 1–10.

Zhang, G., Shen, R., Luo, R., Cao, Y. & Zhang, X. 2010 Effects of sediment load on hydraulics of overland flow on steep slopes. *Earth Surface Processes and Land-Forms* **35** (15), 1811–1819.

Zhang, K. D., Wang, G. Q., Sun, X. M. & Wang, J. J. 2014 Hydraulic characteristic of overland flow under different vegetation coverage. *Advances in Water Science* **25** (6), 825–834.

Zhang, S. T., Zhang, J. Z., Liu, Y. C., Liu, Y. & Wang, Z. K. 2018 The effects of vegetation distribution pattern on overland flow. *Water and Environment Journal* **32**, 392–403.

Zhao, C. H., Gao, J. E., Zhang, M. J., Wang, F. & Zhang, T. 2015 Sediment deposition and overland flow hydraulics in simulated vegetative filter strips under varying vegetation covers. *Hydrological Processes* **30** (2), 163–175.

Zheng, Z. C., He, S. Q. & Wu, F. Q. 2012 Relationship between soil surface roughness and hydraulic roughness coefficient on sloping farmland. *Water Science and Engineering* **5** (2), 191–201.

Zhu, H., Zhao, Y. & Liu, H. 2018 Scale characters analysis for gully structure in the watersheds of loess landforms based on digital elevation models. *Frontiers of Earth Science* **12** (2), 431–443.

First received 25 October 2019; accepted in revised form 30 March 2020. Available online 15 April 2020

Downloaded from http://iwa.silverchair.com/ws/article-pdf/20/4/1463/704790/ws020041463.pdf
by guest